Van Der Waals versus Hydrogen-Bonding in Complexes of Indole with Argon, Water, and Benzene by Mass-Analyzed Pulsed Field Threshold Ionization

J. E. Braun, Th.L. Grebner,† and H. J. Neusser*

Institut für Physikalische und Theoretische Chemie, Technische Universität München, Lichtenbergstrasse 4, D-85748 Garching, Germany

Received: January 6, 1998

By using the technique of mass-analyzed threshold ionization spectroscopy, we were able to measure ionization energies of indole−Ar (62505 cm^{-1}), indole−H_2O (59433 cm^{-1}), and the indole−benzene (59833 cm^{-1}) complexes, as well as their dissociation energies in the cationic ground state. The dissociation energies in the neutral ground state are calculated from the experimental data. The ionic $E_0 = 537 \pm 10$ cm^{-1} and neutral dissociation energy $D_0 = 451 \pm 15$ cm^{-1} of the indole−Ar complex are much smaller than those of the indole−H_2O complex; $E_0 = 4790 \pm 10$ cm^{-1}, $D_0 = 1632 \pm 15$ cm^{-1} and of the indole−C_6H_6 complex: $E_0 = 4581 \pm 10$ cm^{-1}, $D_0 = 1823 \pm 15$ cm^{-1}. This demonstrates the van der Waals character of the indole−Ar complex and the hydrogen bonding type in indole−water. Furthermore, we conclude that the indole−benzene complex is hydrogen-bonded with the benzene π-cloud serving as electron donator and indole serving as hydrogen donator.

1. Introduction

Hydrogen bonding plays an important role in a great variety of physical, chemical, and biological phenomena. One of the most prominent effects caused by hydrogen bonding are the special properties of water which are fundamental for life as we know it. Consequently, a large number of experimental and theoretical studies have been carried out in order to gain information on hydrogen bonds (see e.g., ref 1 and references therein). On the contrary, little experimental information on the dissociation energy of water bound to single polyatomic molecules (i.e., isolated hydrogen-bonded complexes in the gas phase) is available. Recently, optical spectroscopy, combined with mass spectrometry, has been employed by several groups. Leutwyler and co-workers measured the neutral ground-state binding energy of 1-naphthol−H_2O ($D_0 = 2035 \pm 69$ cm^{-1}) using a resonant two-photon two-color pump/dump scheme followed by a two-photon one-color resonantly enhanced ionization.[2] This method probes dissociation of the complex in the neutral ground state but does not provide information on the ionic state. Cheng et al. obtained ionic and neutral ground-state binding energies of benzene−H_2O ($E_0 = 4.0 \pm 0.4$ kcal mol^{-1}, 1399 ± 140 cm^{-1}; $D_0 = 2.25 \pm 0.28$ kcal mol^{-1}, 787 ± 98 cm^{-1}) by comparing one-photon ionization efficiency curves recorded with different gas mixtures, which leads to a variation in the ratio of the benzene monomer to the benzene−H_2O complex.[3] In contrast to the complexes mentioned above, binding of water to benzene has van der Waals character rather than hydrogen-bonding character, because benzene is of hydrophobic nature.[4] In recent work we have demonstrated that the dissociation of van der Waals complex ions can be monitored with the technique of mass analyzed threshold ionization (MATI) as a function of its selected internal energy by a simultaneous observation of threshold ions at the cluster ion mass channel and the fragment ion mass channel.[5,6] MATI spectroscopy is based on the excitation of high ($n \approx 150$) long-lived Rydberg states and their subsequent ionization in a delayed pulsed electric field leading to threshold ions in well-defined energy states.[7] Rydberg states appear in series converging to the various states of the cation. By suppression of nonenergy-selected (prompt) ions, this technique allows us to precisely determine the internal energy of the molecular and complex ions under investigation. For exciting laser light of ≈ 0.3 cm^{-1} bandwidth and a separation field of 0.6 V/cm used in the present experiments, the threshold ion peaks in the MATI spectra indicate the energetic position of vibrational states of the cation within ± 5 cm^{-1} precision. Further on, with the MATI technique it is possible to detect any mass change of the ionic core after the excitation process due to its mass selectivity. Using this technique, we were able to find accurate values for the dissociation energy of several van der Waals complexes of polyatomic molecules with noble gases.[8] For the case of fluorobenzene−Ar we have demonstrated that the measured value of the dissociation threshold depends on the applied ionization field.[9] The reason for this is a coupling of the originally excited high Rydberg states to lower Rydberg states which belong to a series converging to a vibrational state above the dissociation threshold and whose detection needs a higher electric ionization field. By extrapolation of the measured threshold to field zero, we were able to determine the field-free dissociation threshold assuming a square root dependence of the ionization width from the ionizing field. As a consequence, the energetic position of the breakdown of signal in the spectrum measured at the cluster ion mass channel corresponds to the field-free dissociation threshold if there are ionic states close below and above the field-free dissociation threshold.[9] This is the case for the complexes examined in this work. Previous resonantly enhanced multiphoton ionization (REMPI) measurements of ionization efficiency curves of indole complexes involving polar and nonpolar complex partners yielded information on ionization energies and transition energies of neutral excited levels.[10] More recently, vibrational spectra of

† Present address: Labor für Organische Chemie, ETH-Zürich, Universitätsstr. 16, 8092 Zürich, Switzerland.

S1089-5639(98)00649-5 CCC: $15.00
Published on Web 04/22/1998

indole up to ≈1500 cm^{-1} ion internal energy obtained by zero kinetic energy electron pulsed field ionization (ZEKE-PFI) spectroscopy[11] have been reported.[12] These authors asigned several totally and nontotally symmetric modes in the cationic ground state, and a vibrational spectrum around the cationic origin of the indole−Ar van der Waals complex is presented. In the present work we report on the first determination of the dissociation threshold of a hydrogen-bonded ionic complex using a highly sensitive MATI detection scheme. We determine the adiabatic ionization energy and the dissociation energies of the neutral and the ionic indole−H_2O complex with high accuracy. We also performed measurements on the van der Waals bound indole−Ar complex, and we compare the results with findings of our previous work on complexes of Ar with other aromatic systems. Furthermore, we were able to measure ionic spectra and the dissociation threshold of indole−benzene clusters with benzene as a prototype of a large organic molecule involved in the clustering process.

2. Experimental Section

The experimental setup used was described in detail elsewhere.[13] Briefly, it consists of two dye lasers yielding ≈10 ns light pulses with a bandwidth of ≈0.3 cm^{-1} (FL 3002, and LPD 3000; Lambda Physik). The dye lasers are pumped synchronously by an XeCl excimer laser (EMG 1003i, Lambda Physik). The two counter propagating laser beams intersect a skimmed supersonic molecular beam perpendicularly 15 cm downstream from the nozzle orifice. The light pulses overlap in time and space in the ion optics of a linear reflecting time-of-flight mass spectrometer.[14] The supersonic jet is obtained by expanding indole vapor which is produced inside a heated (110 °C) pulsed (25 Hz) valve and seeded into either pure Ar carrier gas (≈3 bar), a mixture of Ne (≈3 bar) and ≈25 mbar H_2O vapor, or a mixture of Ne (≈3 bar) and ≈20 mbar benzene vapor into the vacuum. The excitation of indole or its clusters to high Rydberg levels is achieved by a resonantly enhanced two-photon two-color process. Promptly produced cations originating from a one-color, or two-color, two-photon ionization process or a prompt ionization of molecules excited to Rydberg levels are separated from molecules in long-lived high Rydberg states. This is performed by a delayed pulsed electric field (separation field, ≈0.6 V/cm), which is applied to the first zone (30 mm wide) of the ion optics, in a way that the prompt ions are decelerated. The separation field is switched on about 100 ns after the occurrence of the two laser pulses.[15,16] Within several microseconds the neutral high Rydberg molecules drift into the second zone (20 mm wide) where no electric field is present at that time. An ionization field of 500 V/cm is switched on 28 μs after the occurrence of the two exciting/ionizing laser pulses and ionizes the high Rydberg molecules. The resulting threshold ions are accelerated toward the ion reflector by this electric field and are reflected toward the multichannel plates. Threshold and REMPI spectra are recorded mass selectively with a gated integrator/microcomputer system.

3. Results and Discussion

Indole−Ar Complex. Using the MATI technique described above, a threshold ion spectrum of bare indole (117 u) was recorded and is shown in the bottom trace of Figure 1. It was measured with the frequency of the first laser fixed to the S_1 (^1L_b) ← S_0, 0^0_0 transition at 35231 cm^{-1}. The assignments are adopted from refs 17−19. A threshold ion spectrum of the indole−Ar van der Waals (vdW) complex (157 u, parent spectrum) is shown in the middle trace of Figure 1. (Threshold

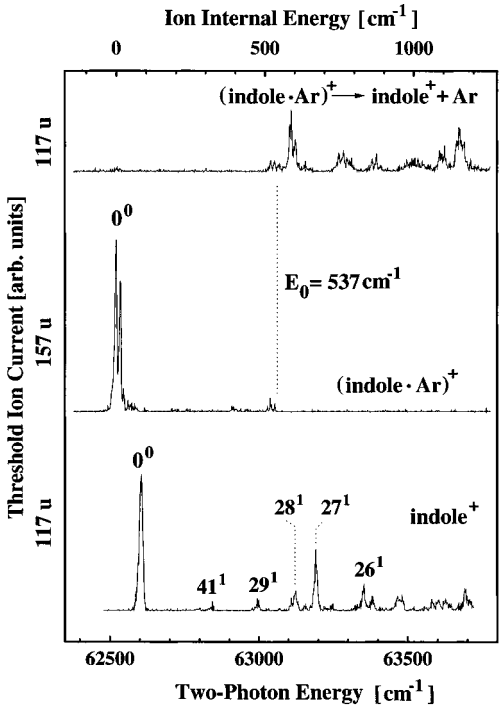

Figure 1. Threshold ion spectrum of indole−Ar at mass channel 117 u (top) and 157 u (middle) measured by a two-color two-photon excitation precess with the first photon energy fixed to the vibrationless S_1 origin. Bottom: Threshold ion spectrum of the bare indole molecule. The broken line indicates the position of the field-free ionic dissociation threshold at $E_0 = 537 \pm 10$ cm^{-1}.

ion spectra of the cluster recorded at the parent mass channel are denoted "parent spectra" and spectra recorded at the mass channel of the charged dissociation product of the cluster are denoted "daughter spectra"). It was recorded with the frequency of the first laser fixed to the red-shifted S_1 (^1L_b) ← S_0, 0^0_0 transition at 35205 cm^{-1}. The origin of the vdW cluster threshold ion spectrum is located at 62505 ± 5 cm^{-1} and shifted by 86 cm^{-1} to the red of the bare molecule origin (62591 ± 5 cm^{-1}). The origin band of the complex cation shows additional low-frequency vibrational structure with four members of a progression with ≈14 cm^{-1} spacing. This arises from the excitation of a bending vdW mode and was also observed by Kimura and co-workers using ZEKE-PFI spectroscopy.[12] Similar signatures are known from complexes of Ar with other aromatic molecules.[20−24] The spectrum on top of Figure 1 represents the daughter ion spectrum (117 u) of indole−Ar which was recorded simultaneously with the parent threshold ion spectrum (middle trace, 157 u) for the same excitation conditions. Breakdown of signal in the parent spectrum is observed for ion internal energies exceeding 537 cm^{-1} (dotted line) in an ion internal energy region with dense vibrational structure. On the other hand, signal appears in the daughter spectrum for ion internal energies exceeding 487 cm^{-1}. An important result is the observed overlap of ≈50 cm^{-1} of the parent and the daughter spectrum between 487 and 537 cm^{-1} excess energy. In this internal energy range, part of the clusters dissociate, whereas the other part remains stable. As discussed in previous work[9] this behavior is caused by a coupling of *high* Rydberg levels converging to ionic states *below* the field-free dissociation threshold to *lower* Rydberg levels converging to ionic states *above* the field-free dissociation threshold. As a consequence energy is transferred from the electronically excited high Rydberg electron to the vibrational degrees of freedom of the cluster ion core. If the coupled states are within the ranges of Rydberg states which can be ionized by the ionization field

TABLE 1: Experimental Values for Neutral Ground-State D_0 and Ionic E_0 Dissociation Thresholds of the Three Complexes Examined in This Work Together with Their Adiabatic Ionization Energies (AIE) and $S_1 \leftarrow S_0$, 0_0^0 Transition Energies

	$S_1 \leftarrow S_0$, 0_0^0	AIE (cm^{-1})	E_0 (cm^{-1})	D_0 (cm^{-1})	D_0 (kJ/mol)
indole	35 231	62 591			
indole−Ar	35 205	62 505	537	451 ± 15	5.39 ± 0.18
indole−H_2O	35 099	59 433	4790	1632 ± 15	19.52 ± 0.18
indole−C_6H_6	35 067	59 833	4581	1823 ± 15	21.8 ± 0.18

(500 V/cm, ionization down to ≈ 87 cm^{-1}, $n \approx 36$) signal appears in the daughter spectrum although the energy deposited in the cluster ion core by the optical excitation is below the field-free dissociation threshold. In recent work, we determined the field-free dissociation threshold by extrapolation of the dissociation threshold to zero field and found that it agrees with the breakdown threshold of the parent ion signal. As a result we concluded that the breakdown of signal in the parent trace is more important for the assignment of the field-free dissociation threshold than the onset of signal in the daughter trace. According to these findings, we obtain a dissociation energy of $E_0 = 537 \pm 10$ cm^{-1} for the ionic indole−Ar complex. The dissociation threshold in the neutral ground state is calculated to $D_0 = E_0 - (AIE_{indole} - AIE_{indole-Ar}) = 451$ cm^{-1}. (AIE = adiabatic ionization energy.) (See Table 1.) This value is slightly smaller than the theoretical value $D_0 = 480$ cm^{-1} obtained by Hager et al. and is in line with their experimental upper limit of 528 cm^{-1}.[25] The neutral ground-state dissociation threshold D_0 of indole−Ar lies between the measured binding energies of Ar to one-ring substrates such as oxazole with $D_0 = 304$ cm^{-1} (ab initio),[26] benzene with $D_0 \leq 340$ cm^{-1} (experimental)[6] and $D_0 = 337$ cm^{-1} (ab initio),[26] fluorobenzene with $D_0 = 346 \pm 10$ cm^{-1} (experimental),[9,27] and three-ring substrates such as carbazole with D_0 530.4 ± 1.5 cm^{-1} (experimental),[28] dibenzo-*p*-dioxin with $D_0 = 527 \pm 18$ cm^{-1} (experimental),[8] and dibenzofuran with $D_0 = \leq 521 \pm 12$ cm^{-1} (experimental).[8] These findings show that the binding energy of a single Ar atom to neutral aromatic molecules in the ground state is governed by the number of aromatic rings in the substrate for the same arrangement of the aromatic rings, whereas the influence of heteroatoms in the substrate appears to be small. With increasing ring number, the binding energy converges to the adsorption energy of Ar bound to the (001) surface of graphite, which is ≈800 cm^{-1}.[29]

Indole−H_2O Complex. *Intermediate State Spectra.* The $S_1 \leftarrow S_0$ intermediate state spectra of indole and indole−H_2O recorded by resonantly enhanced two-photon two-color ionization (REMPI) are shown in Figure 2. A high-resolution $S_1 \leftarrow S_0$ intermediate state spectrum with rotational fine structure is reported in the accompanying paper from our group.[31] Information on the structure of indole−H_2O with indole serving as hydrogen donor was achieved by simulation in an asymmetric top fit of the measured spectrum. This simulation yields that the oxygen atom of the water moiety is located in the plane of the indole molecule 2.9 Å away from the H-atom of the indole >N−H group. The spectroscopical assignments for indole are adopted from refs 17−19. In case of indole−H_2O, assignments are given by assuming small shifts of the intramolecular vibrational bands to the red. In addition to bare indole, two low-frequency transitions appear at 25 cm^{-1} (β) and 128 cm^{-1} (σ) blue shifted from the origin of the complex, which are most likely of intermolecular nature. Hager et al. found two different origins in the $S_1 \leftarrow S_0$ spectrum of the 1:1 complex of water and indole and assigned them to two different conformers.[10]

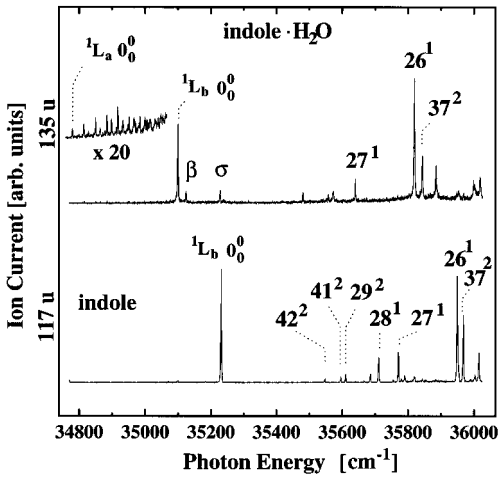

Figure 2. $S_1 \leftarrow S_0$ spectra of indole−H_2O (top) and indole (bottom) measured by resonantly enhanced two-color two-photon ionization. ^1L_b 0^0_0 is the origin of the $S_1 \leftarrow S_0$ spectrum of the indole−H_2O conformer with indole serving as an hydrogen donator. The weaker ^1L_a 0^0_0 transition is seen on the spectrum with the magnified intensity scale on the red side of the ^1L_b transition.

Later, Tubergen and Levy proposed that solvents accepting a hydrogen bond are attached via the hydrogen of the N−H group of indole and do not change the order of the lowest electronically excited states (^1L_b and ^1L_a) of indole[30] (i.e., the ^1L_b state remains the first electronically excited state in this case). On the other hand, solvents that are able to donate a hydrogen bond to the indole π-cloud lower the ^1L_a state according to their dipole moment and due to specific bonding properties so that the order of the lowest electronically excited states is reversed. For water as solvent the hydrogen bonded complex with indole serving as hydrogen donor has its ^1L_b origin at 35099 cm^{-1} (35104 cm^{-1}[30]) which is red shifted 132 cm^{-1} away from the bare molecule ^1L_b origin. The progressions to the red of the ^1L_b origin (shown in the magnified upper scale on the left of Figure 2) of the hydrogen bonded complex with indole serving as hydrogen donor were attributed to low-frequency modes of the second conformer whose ^1L_a origin is at 34780 cm^{-1} (34782 cm^{-1}[30]), red shifted by 451 cm^{-1} away from the lowest (^1L_b) origin of the bare indole molecule. Under the jet conditions of our experiment, the complex with indole serving as hydrogen donor is predominantly produced and denoted as indole−H_2O in the following text.

Mass Analyzed Threshold Ionization Spectra. The threshold ion spectrum of bare indole (117 u) was recorded by resonance-enhanced two-photon excitation with the first laser frequency fixed to the S_1 (^1L_b), 0° intermediate state. It is shown in Figure 3 (top). For comparison, this spectrum and the lower three threshold ion spectra of the indole−H_2O complex are displayed on a common ion internal energy scale, though the absolute excitation energy is different for the monomer and the cluster spectra. The prominent peak at the lowest two-photon energy of 62591 ± 5 cm^{-1} corresponds to the AIE of indole (AIE, 0°) (62592 ± 4 cm^{-1},[12] 62598 ± 5 cm^{-1} [10]). The assignments of the vibrational states of the indole cation are taken from ref 12. Threshold ion spectra of indole−H_2O obtained via three different intermediate states are shown in the lower three traces of Figure 3. As we can clearly identify intramolecular modes in the complex spectrum after a comparison with indole trace, the adiabatic ionization energy of the complex is unambiguously given by the first peak in the threshold ion spectrum at 59433 ± 5 cm^{-1}. It is red shifted by 3158 ± 5 cm^{-1} away from the bare indole origin. This differs

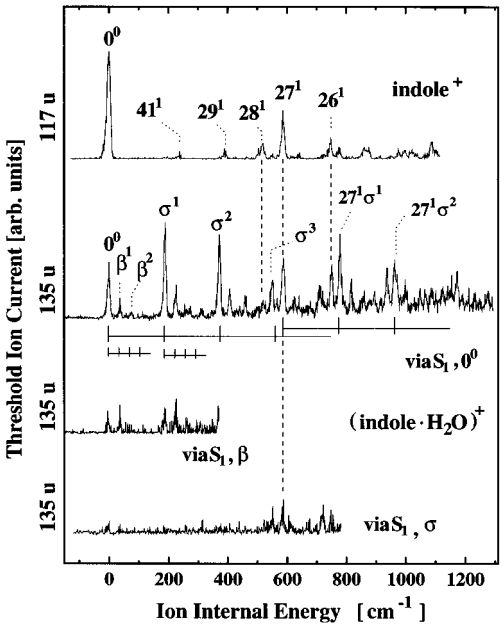

Figure 3. Threshold ion spectrum of indole (top) and three threshold ion spectra of indole−H_2O measured via different intermediate state transitions. All spectra are scaled to ion internal energies. The uppermost indole−H_2O spectrum is obtained via pumping the vibrationless intermediate state origin S_1, 0°. The lower two spectra are obtained by pumping the low-frequency bands denoted β and σ in the intermediate state spectrum of indole−H_2O (see Figure 2).

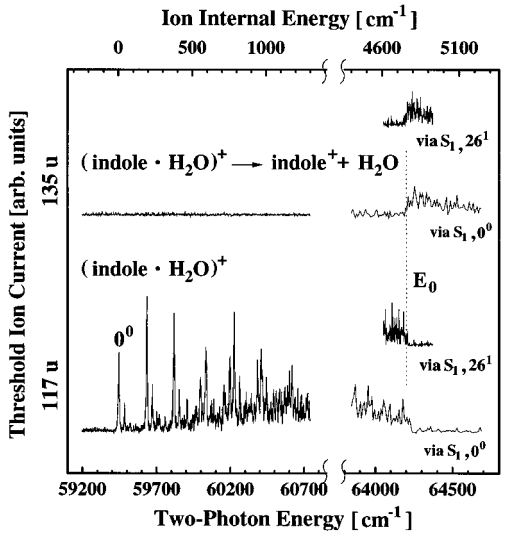

Figure 4. Left: Two threshold ion spectra of indole−H_2O measured at low (<1300 cm^{-1}) ion internal energy at the daughter mass, 117 u (top), and the parent mass, 135 u (bottom). The intermediate state is the vibrationless intermediate state origin ^1L_b. Right: Two sets of threshold ion spectra of indole−H_2O measured at high ion internal energies at the daughter mass, 117 u (upper two spectra), and the parent mass, 135 u (lower two spectra), respectively. The upper spectra in both sets are obtained by pumping via the 26^1 intermediate state transition, and the lower two spectra are obtained via pumping the vibrationless intermediate state origin. The broken line indicates the field-free dissociation threshold which occurs at the same ion internal $E_0 = 4790 \pm 10$ cm^{-1} energy in both sets (For explanation, see text).

by 131 cm^{-1} from the value given in ref 10 obtained with photoionization efficiency (PIE) spectroscopy. The uppermost spectrum of the three complex spectra in Figure 3 was measured via the vibrationless intermediate state origin S_1, 0°. It is dominated by progressions of two vibrational modes. A strong progression with 189 cm^{-1} spacing (σ^1) is observed originating at the vibrationless origin 0° of the complex as well as at the 27^1 mode. In addition, a weak progression with 38 cm^{-1} spacing (β^1) originating at several vibrational bands is observed. The strong progression is tentatively assigned to the stretching mode which is supposed to form long progressions in the ionic spectra because strengthening of the binding between water and indole upon ionization leads to a reduction of the hydrogen bonding length and larger Franck−Condon factors for $\Delta\nu > 1$ transitions. The existence of long progressions is similar to the finding in the ZEKE-PFI spectra of the phenol−water complex.[32] Additionally, an anharmonicity in the ionic σ-progression can be observed. The energy differences of the first, second, and third quantum are 189, 183, and 180 cm^{-1}, respectively. The lower two traces in Figure 3 represent threshold ion spectra of indole−H_2O obtained by pumping via the two low-frequency intermediate state transitions denoted with σ and β in Figure 2. The spectrum obtained via S_1,β shows an enhancement of the first quantum of the ionic β progressions. This confirms the assignment of this progression to the β mode which has been identified in the S_1 state. Because of low signal intensity, the spectrum obtained by excitation via the S_1,σ state is noisy (bottom trace of Figure 3), with the σ^3 band as the most intensive feature. The frequency of the ionic σ and β progressions is larger by 50% than the respective frequencies in the intermediate state. This is due to the increased strength of the hydrogen bonding in the ionic state caused by the additional charge−dipole interaction.

Dissociation Energy. Next we recorded parent and daughter threshold ion spectra of indole−H_2O in a higher ion internal energy range. On the left side of Figure 4 the parent ion spectrum (bottom) and the daughter ion spectrum (top) of indole−H_2O are shown, recorded simultaneously in the range from zero up to 1300 cm^{-1} ion internal energy after pumping via the vibrationless S_1, 0° origin. The parent ion spectrum shows long progressions of the σ mode which has been discussed above (see Figure 3). No signal is observed on the daughter trace and hence no dissociation takes place in this spectral range. On the right side of Figure 4 two parent (lower set) and two daughter spectra (upper set) in an ion internal energy range from 4400 to 5250 cm^{-1} are displayed, obtained by pumping via the vibrationless S_1, 0° origin and the 26^1 intermediate state transition, respectively. Both parent spectra show a breakdown and both daughter spectra an appearance of signal at the same ion internal energy although this energy level has been reached via different intermediate states. This means that no mode selectivity of the dissociation energy is observed and we expect a statistical distribution of energy to all vibrational degrees of freedom before dissociation. The ion signal rises or decreases within 35 cm^{-1} to the final level, and again, an overlap of the parent and daughter traces, such as in indole−Ar, is observed. The range of overlap is somewhat smaller than expected for energy transfer to the low Rydberg states (n = 50) that can be ionized by the delayed ionization field of 500 V/cm if we assume that around 5000 cm^{-1} above the ionic origin the density of accessible states can be considered as quasi continuous. This might be a consequence of a shorter lifetime of low Rydberg states due to the dipole moment of the ion core which is larger than, for example, in the case of indole−Ar. From the breakdown of signal in the parent trace we find a field-free dissociation threshold $E_0 = 4790 \pm 10$ cm^{-1} and the dissociation threshold in the neutral ground state is calculated to $D_0 = E_0 - (AIE_{indole} - AIE_{indole-H_2O}) = 1632 \pm 15$ cm^{-1}. Recently, the binding energy of water to neutral 1-naphthol was measured by Bürgi et al. yielding $D_0 = 2035 \pm 69$ cm^{-1} [2]. This is higher by 400 cm^{-1} than the value found in this work for the

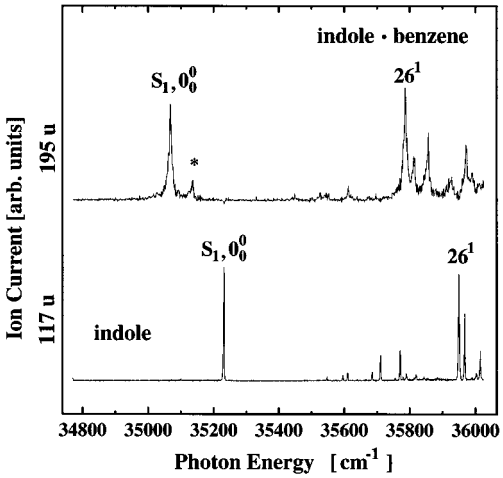

Figure 5. $S_1 \leftarrow S_0$ intermediate state spectra of indole−benzene (top) and indole (bottom) measured by resonantly enhanced two-color two-photon ionization. The peak marked by an asterisk is explained in the text.

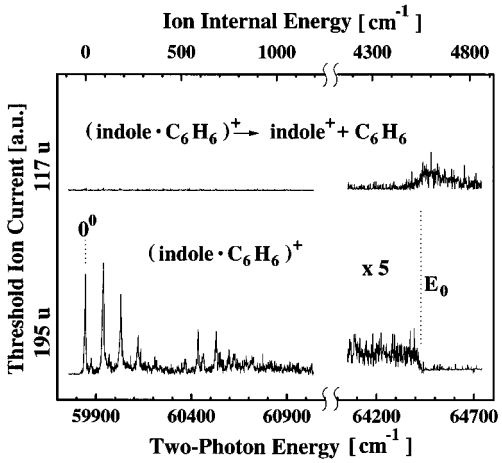

Figure 6. Threshold ion spectra of indole−benzene measured from 0 up to 1200 cm^{-1} ion internal energy (left) and from 4200 cm^{-1} up to 4900 cm^{-1} ion internal energy (right) at the daughter mass, 117 u (top), and the parent mass, 195 u (bottom). The spectra are obtained by pumpinging the vibrationless intermediate state origin. The broken line indicates the field-free dissociation threshold at an ion internal energy of $E_0 = 4581 \pm 10$ cm^{-1}.

binding energy of water to indole and is in line with the general rule that a >N−H···O< type hydrogen bond is weaker than a >O−H···O< type hydrogen bond present, for example, in the naphthol−water complex.

Indole−Benzene Complex. It has been shown that molecules containing an acidic hydrogen can form a π-hydrogen bond with an aromatic molecule.[20,36,40,41] Consequently, it was argued by Hager at al. that the 1:1 complex of indole and benzene is most likely bound by the formation of a hydrogen bond[10] such as that in indole−H_2O discussed in the previous section. Their conclusion was based on the experimental red shift of the S_1, 0^0_0 origin. Complexation with a single benzene shifts the intermediate state origin of indole by − 166 cm^{-1}, whereas the complexation with a second benzene molecule give rise to only − 17 cm^{-1} additional red shift. This is a clear hint that the binding site of the second benzene is significantly different from the binding site of the first benzene molecule. Since indole has one acidic hydrogen, only a single benzene molecule can be bound by a π-hydrogen bond. Thus, the second benzene in the indole−$(benzene)_2$ complex is bound by pure van der Waals interaction leading to the observed smaller shift of the electronic transition. In this work we investigate the binding strength of the indole−benzene complex which is expected to yield direct information on the type of the binding.

Intermediate State Spectrum. The intermediate state spectrum of indole−benzene is shown in the upper part of Figure 5 (top) and compared with the indole monomer spectrum (lower trace). It displays a structure similar to the bare indole spectrum with the S_1, 0^0_0 origin and the 26^1_0 band as the strongest peaks. The S_1, 0^0_0 origin of the complex is located at 35067 cm^{-1} and red shifted 165 cm^{-1} away from the bare molecule origin. An additional band, which is not present in the monomer spectrum, appears at 34.5 cm^{-1} to the blue of the S_1, 0° cluster origin and is marked with an asterisk. We did not see any features of indole−$(benzene)_2$ at mass 273 u at this frequency. Therefore, we assign this band to the first quantum of an intermolecular vibration of the 1:1 complex. Most likely this is an intermolecular vibration with stretching character. The typical width (fwhm) of the peaks in the cluster spectrum is ≈6.5 cm^{-1}, which is broader by a factor of 2 compared to the corresponding peaks in the monomer spectrum. Most likely this is due to the excitation of low-frequency vibrations of the complex with are not resolved.

Mass Analyzed Threshold Ionization Spectra. On the left side of Figure 6 the parent threshold ion spectrum (lower trace) and the daughter threshold ion spectrum (upper trace) of indole−C_6H_6 at low internal energy (<1000 cm^{-1}) are shown. The AIE is found to be 59833 ± 5 cm^{-1} and thus red shifted by −2785 ± 5 cm^{-1} away from the bare indole AIE. The assignment of the AIE is corroborated by arguments similar to the case of the indole−H_2O complex (see above). The threshold ion spectrum of indole−C_6H_6 is dominated by a long progression with 95 cm^{-1} spacing. This spacing is approximately half the spacing of the long progression in (indole−H_2O)$^+$. This is what we expect for an intermolecular vibration with stretching character when taking into account the higher mass of the benzene moiety. As demonstrated below, the binding strength is similar in both systems.

Dissociation Energy. On the left sige of Figure 6 the parent and daughter threshold ion spectra of indole−C_6H_6 at large ion internal energies is displayed. The parent signal (lower trace) breaks down at 4581 ± 10 cm^{-1} ion internal energy. At roughly the same energy an onset of the daughter signal is observed. Therefore, the dissociation threshold of the (indole−C_6H_6)$^+$ complex is located at $E_0 = 4581 \pm 10$ cm^{-1} and the dissociation threshold in the neutral ground state is calculated to $D_0 = 1823 \pm 15$ cm^{-1}. The observed decrease of signal in the daughter trace with increasing ion internal energy is caused by the decreasing laser pulse energy in this spectral range. The neutral binding energy of indole−C_6H_6 is much larger than the binding energies of mixed and homogeneous dimeric complexes of aromatic molecules, such as benzene, *p*-difluorobenzene, and toluene. For these dimers experimental[14,33−37] and in part theoretical values[34,38,40] obtained by various methods have been found. The complex studied most intensive is the benzene dimer for which recent ab initio calculations demonstrated that the parallel-displaced (PD) and the T-shaped (T) structure have nearly the same stabilization energy of about 2.3 kcal/mol (800 cm^{-1}).[38] (Note that the zero point energy has to be subtracted to obtain the dissociation energy.) Breakdown measurements yielded 566 ± 80 cm^{-1} for the benzene homo dimer and 645 ± 120 cm^{-1} for the *p*-difluorobenzene−benzene as well as the toluene−benzene hetero dimers.[39] Even if one takes into account that indole is larger than any of the dimers mentioned above, the factor of 2 larger binding energy of the indole−C_6H_6 complex cannot be explained by the resulting larger van

der Waals interaction only. From this we conclude that the interaction is dominated by hydrogen bonding involving the >N−H group of indole and the benzene π-cloud serving as an electron donator.

4. Summary and Conclusion

In this work we presented the first threshold ion (MATI) spectrum of a hydrogen-bonded complex. We found accurate values for microscopic binding energies for the hydrogen bond in the indole−H_2O complex in the neutral and the cationic ground state. The neutral binding energy of indole−H_2O is 4 times larger than the pure van der Waals binding energy in the indole−Ar complex. For indole−C_6H_6, hydrogen-bonding character of the binding is concluded from the large dissociation energies in the neutral and ionic ground states. Additionally, information on the intermolecular vibrational dynamics of hydrogen bonds in the ionic complexes was obtained. Weak interactions between molecules (van der Waals and hydrogen bond) play an important role in the formation of the tertiary (3-D) structure of proteins and peptides. The energetics of hydrogen bonding is therefore basic information for the explanation of structure and functionality of biomolecules, such as enzymes, etc. The hydrogen bond of the type >N−H···O< present in the indole−H_2O complex is of particular interest because indole is a basic component of the amino acid tryptophane, which is one of the 20 natural amino acids found in living beings. The indole molecule also provides the basic structure of serotonine, one of the nine known neurotransmitters which are responsible for the chemical information exchange between neurons. The energetics and intermolecular dynamics of hydrogen bonds between indole and water and organic molecules, such as benzene, respectively, has prototype character for the understanding of the more complex biological systems. Furthermore, the latter complex is particularly interesting because its excitation appears to be feasible by employing either the indole or the other moiety as a chromophore. This may provide valuable information on intracluster electron-transfer reactions soon.

Acknowledgment. Financial support from the Deutsche Forschungsgemeinschaft and the Fonds der Chemischen Industrie is gratefully acknowledged.

References and Notes

(1) Huyskens, P. L., Luck, W. A. P., Zeegers-Huyskens,T., Eds. *Intermolecular Forces*; Springer-Verlag: Berlin, 1991.
(2) Bürgi, T.; Droz, T.; Leutwyler, S. *Chem. Phys. Lett.* **1995**, *246*, 291.
(3) Cheng, B.-M.; Grover, J. R.; Walters, E. A. *Chem. Phys. Lett.* **1995**, *232*, 364.
(4) Gotch, A. J.; Zwier, T. S. *J. Chem. Phys.* **1992**, *96*, 3388.
(5) Krause, H.; Neusser, H. J. *J. Chem. Phys.* **1992**, *97*, 5923.
(6) Krause, H.; Neusser, H. J. *J. Chem. Phys.* **1993**, *99*, 6278.
(7) Zhu, L.; Johnson, P. M. *J. Chem. Phys.* **1991**, *94*, 5769.
(8) Grebner, Th. L.; Stumpf, R.; Neusser, H. J. *Int. J. Mass Spectrom. Ion Processes* 1988. In press.
(9) Grebner, Th. L.; Unold, P. v.; Neusser, H. J. *J. Phys. Chem. A* **1997**, *101*, 158.
(10) Hager, J.; Ivanco, M.; Smith, M. A.; Wallace, S. C. *Chem. Phys.* **1986**, *105*, 397.
(11) Reiser, G.; Habenicht, W.; Müller-Dethlefs, K.; Schlag, E. W. *Chem. Phys. Lett.* **1988**, *152*, 119.
(12) Vondrak, T.; Sato, S.; Kimura, K. *J. Phys. Chem.* **1997**, *101*, 2348.
(13) Grebner, Th. L.; Neusser, H. J. *Chem. Phys. Lett.* **1995**, *245*, 578.
(14) Ernstberger, B.; Krause, H.; Kiermeier, A.; Neusser, H. J. *J. Chem. Phys.* **1990**, *92*, 5285.
(15) Merkt, F. *J. Phys. Chem.* **1994**, *100*, 2623.
(16) Dietrich, H. J.; Lindner, R.; Müller-Dethlefs, K. *J. Chem. Phys.* **1994**, *101*, 3399.
(17) Nibu, Y.; Abe, H.; Mikami, N.; Ito, M. *J. Phys. Chem.* **1983**, *87*, 3898.
(18) Bickel, G. A.; Demer, D. R.; Outhouse, E. A.; Wallace, S. C. *J. Chem. Phys.* **1989**, *91*, 6013.
(19) Barstis, T. L. O.; Grace, L. I.; Dunn, T. M.; Lubman, D. M. *J. Phys. Chem.* **1993**, *97*, 5820.
(20) Xu Zhang, Smith, J. M.; Knee, J. L. *J. Chem. Phys.* **1992**, *97*, 2843.
(21) Takahashi, M.; Ozeki, H.; Kimura, K. *J. Chem. Phys.* **1992**, *96*, 6399.
(22) Cockett, M. C. R.; Okuyama, K.; Kimura, K. *J. Chem. Phys.* **1992**, *97*, 4679.
(23) Grebner, Th. L.; Neusser, H. J. *Int. J. Mass Spectrom. Ion Processes* **1996**, *159*, 137.
(24) Shinohara, H.; Sato, S.; Kimura, K. *J. Phys. Chem.* **1997**, *101*, 6736.
(25) Outhouse, E. A.; Bickel, G. A.; Demmer, D. R.; Wallace, S. C. *J. Chem. Phys.* **1991**, *95*, 6261.
(26) Kraka, E.; Cremer, D.; Spoerel, U.; Merke, I.; Stahl, W.; Dreizler, H. *J. Phys. Chem.* **1995**, *99*, 12466.
(27) Lembach, G.; Brutschy, B. *J. Chem. Phys.* **1997**, *107*, 6156.
(28) Droz, T.; Bürgi, T.; Leutwyler, S. *J. Chem. Phys.* **1995**, *103*, 4035.
(29) Steele, W. A. *Surf. Sci.* **1973**, *36*, 317.
(30) Tubergen, M. J.; Levy, D. H. *J. Phys. Chem.* **1991**, *95*, 2175.
(31) Helm, R. M.; Clara, M.; Grebner, Th. L.; Neusser, H. J. *J. Phys. Chem.* **1998**. xxxx
(32) Dopfer, O.; Reiser, G.; Müller-Dethlefs, K.; Schlag, E. W.; Colson, S. D. *J. Chem. Phys.* **1994**, *101*, 974.
(33) Nishiyama, I.; Hanazaki, I. *Chem. Phys. Lett.* **1985**, *117*, 99.
(34) de Meijere, A.; Huisken, F. *J. Chem. Phys.* **1990**, *92*, 5826.
(35) Meot-Ner, M.; Hamlet, P.; Hunter, E. P.; Field, F. H. *J. Am. Chem. Soc.* **1978**, *100*, 5466.
(36) Kiermeier, A.; Ernstberger, B.; Neusser, H. J.; Schlag, E. W. *J. Phys. Chem.* **1988**, *92*, 3785.
(37) Ernstberger, B.; Krause, H.; Neusser, H. J. *Z. Phys. D* **1991**, *20*, 189.
(38) Hobza, P.; Selzle, H. L.; Schlag, E. W. *J. Phys. Chem.* **1996**, *100*, 18790.
(39) Ernstberger, B.; Krause, H.; Kiermeier, A.; Neusser, H. J. *J. Chem. Phys.* **1990**, *92*, 5285.
(40) van de Waal, B. W. *Chem. Phys. Lett.* **1986**, *123*, 69.
(41) Joesten, M. D. *J. Chem. Educ.* **1982**, *59*, 362.
(42) Abe, H.; Mikami, N.; Ito, M. *J. Phys. Chem.* **1982**, *86*, 1768.
(43) Hager, J.; Wallace, S. C. *J. Phys. Chem.* **1984**, *88*, 5513.